frontiers in Marine Science

ORIGINAL RESEARCH
published: 06 December 2019
doi: 10.3389/fmars.2019.00702

Ocean Circulation Over North Atlantic Underwater Features in the Path of the Mediterranean Outflow Water: The Ormonde and Formigas Seamounts, and the Gazul Mud Volcano

Ángela Mosquera Giménez[1], Pedro Vélez-Belchí[1], Jesús Rivera[2], Safo Piñeiro[3], Noelia Fajar[4], Verónica Caínzos[5], Rosa Balbín[3], Juan Antonio Jiménez Aparicio[3], Carlos Dominguez-Carrió[6], Jordi Blasco-Ferre[6], Marina Carreiro-Silva[6], Telmo Morato[6], Patricia Puerta[3] and Covadonga Orejas[3]*

[1] Centro Oceanográfico de Canarias, Instituto Español de Oceanografía, Santa Cruz de Tenerife, Spain, [2] Servicios Centrales, Instituto Español de Oceanografía, Madrid, Spain, [3] Centro Oceanográfico de Baleares, Instituto Español de Oceanografía, Palma, Spain, [4] Centro Oceanográfico de A Coruña, Instituto Español de Oceanografía, A Coruña, Spain, [5] IOCAG, Universidad de Las Palmas de Gran Canaria, Instituto de Oceanografiia y Cambio Global, ULPGC, Unidad Asociada ULPGC-CSIC, Las Palmas de Gran Canaria, Spain, [6] Marine and Environmental Sciences Centre, Centro OKEANOS, Instituto do Mar, Universidade dos Açores, Horta, Portugal

Seamounts constitute an obstacle to the ocean circulation, modifying it. As a result, a variety of hydrodynamical processes and phenomena may take place over seamounts, among others, flow intensification, current deflection, upwelling, Taylor caps, and internal waves. These oceanographic effects may turn seamounts into very productive ecosystems with high species diversity, and in some cases, are densely populated by benthic organisms, such corals, gorgonians, and sponges. In this study, we describe the oceanographic conditions over seamounts and other underwater features in the path of the Mediterranean Outflow Water (MOW), where populations of benthic suspensions feeders have been observed. Using CTD, LADPC and biochemical measurements carried out in the Ormonde and Formigas seamounts and the Gazul mud volcano (Northeast Atlantic), we show that Taylor caps were not observed in any of the sampled features. However, we point out that the relatively high values of the Brunt–Väisälä frequency in the MOW halocline, in conjunction with the slope of the seamount flanks, set up conditions for the breakout of internal waves and amplification of the currents. This may enhance the vertical mixing, resuspending the organic material deposited on the seafloor and, therefore, increasing the food availability for the communities dominated by benthic suspension feeders. Thus, we hypothesize that internal waves could be improving the conditions for benthic suspension feeders to grow on the slope of seamounts.

Keywords: seamounts, Mediterranean Outflow Water, Taylor columns/caps, internal waves, cold-water corals

OPEN ACCESS

Edited by:
J. Murray Roberts, The University of Edinburgh, United Kingdom

Reviewed by:
Christian Mohn, Aarhus University, Denmark
Rui Caldeira, Agência Regional para o Desenvolvimento da Investigação Tecnologia e Inovação (ARDITI), Portugal

****Correspondence:***
Ángela Mosquera Giménez
angela.mosquera@ieo.es; angela_mosq@hotmail.com

Specialty section:
This article was submitted to Deep-Sea Environments and Ecology, a section of the journal Frontiers in Marine Science

Received: *21 December 2018*
Accepted: *31 October 2019*
Published: *06 December 2019*

Citation:
Mosquera Giménez Á, Vélez-Belchí P, Rivera J, Piñeiro S, Fajar N, Caínzos V, Balbín R, Jiménez Aparicio JA, Dominguez-Carrió C, Blasco-Ferre J, Carreiro-Silva M, Morato T, Puerta P and Orejas C (2019) Ocean Circulation Over North Atlantic Underwater Features in the Path of the Mediterranean Outflow Water: The Ormonde and Formigas Seamounts, and the Gazul Mud Volcano. Front. Mar. Sci. 6:702. doi: 10.3389/fmars.2019.00702

INTRODUCTION

According to the Staudigel et al. (2010) definition, seamounts are any geographically isolated topographic feature taller than 100 m. Either forming clusters or alone, seamounts constitute an obstacle to the free ocean flow, modifying the pattern of circulation not only locally but also globally (Lavelle and Mohn, 2010). As a result of these alterations, a variety of hydrodynamical processes and phenomena, such as flow intensification, current deflection, upwelling, turbulence, trapped waves, jets, Taylor caps, or internal waves, can take place (Noble and Mullineaux, 1989; Eriksen, 1991; Roden, 1991; Dower et al., 1992; Beckmann and Mohn, 2002; Mohn and Beckmann, 2002; Coelho and Santos, 2003). Besides, seamounts play an important role in the generation, breakdown, and even trapping of eddies (Royer, 1978; Roden, 1986; Bashmachnikov et al., 2009; Sokolovskiy et al., 2013).

These oceanographic processes induced by the topography may provoke the enhancement of the primary production and retention of plankton (Xavier and van Soest, 2007; Denda et al., 2016), turning seamounts into ecosystems with high biomass, biodiversity and sometimes with a considerable level of endemism (Boehlert and Genin, 1987; Beckmann and Mohn, 2002; O'Hara, 2007; Pitcher et al., 2007; Clark et al., 2010; Miller and Gunasekera, 2017), which offer particularly good conditions for the settlement of benthic suspension feeders like corals and sponges (Koslow et al., 2001; Xavier and van Soest, 2007; O'Hara et al., 2008). Cold-water corals (CWC) have been described along the path of the Mediterranean Outflow Water (MOW) in several locations: at the Gazul mud volcano (Rueda et al., 2016), the Galicia Bank (e.g., Duineveld et al., 2004; Serrano et al., 2017), and the Porcupine Seabight (De Mol et al., 2002), among others.

The MOW is an intermediate water mass, salty, and warm, found between 800 and 1,500 m depth (Daniault et al., 1994). It is formed when the dense Mediterranean water reaches the Gulf of Cadiz through the Strait of Gibraltar and mixes with the lighter Atlantic water flowing over, forming a less salty water mass (Bozec et al., 2011). After leaving the Gulf of Cadiz, around Cape St. Vincent, the MOW spreads in two directions: northwards, following the continental slopes of the Iberian Peninsula, and westwards, to the central-North Atlantic (Iorga and Lozier, 1999).

Some studies have suggested a possible Mediterranean origin for CWC in the pathway of the MOW through the eastern Atlantic (De Mol et al., 2005; Henry et al., 2014), supported by the stepping stone role largely attributed to seamounts (Brenke, 2002; Gubbay, 2003; Samadi et al., 2006; O'Hara, 2007). However, in spite of the importance of those seafloor elevations for the spread and settlement of CWC and other benthic organisms (Koslow et al., 2001; Brenke, 2002; Gubbay, 2003; Samadi et al., 2006; O'Hara, 2007), there are few studies addressing the ocean circulation and hydrographic conditions over seamounts in the pathway of the MOW.

In this paper, we investigate the role of the hydrographic conditions over several underwater features in the pathway of the MOW to determine the dynamics that likely boost the settlement of benthic suspension feeders in these areas. Specifically, we address whether the well-known Taylor caps are the phenomenon governing the dynamics of the Ormonde and Formigas seamounts and the Gazul mud volcano (**Figure 1**). We also address the importance of the water mass distribution in establishing the dynamical conditions on the slope of these features. We hypothesize that the presence of the MOW lead to relatively high values of the Brunt–Väisälä frequency in its halocline, which, together with the steep slope, will set up conditions for the breakout of internal waves and the amplification of currents at the bottom, favoring the presence of benthic suspension feeders near the seabed.

This paper is organized as follows: the section "Materials and Methods" describes the data acquisition and processing methodology. The section "Results" presents the results of the dynamics and hydrography of each region of study. Lastly, section "Summary and Discussion" summarizes and briefly discusses the results obtained.

MATERIALS AND METHODS

Area of Study

Following the path of the MOW through the eastern Atlantic, three seafloor elevated features, where CWC have been described (WWF, 2004; Oceana, 2005; Rueda et al., 2016), were selected as target regions for this study: the Gazul mud volcano and the Ormonde and Formigas seamounts (**Figure 1**). Both Gazul and Ormonde are directly in the pathway of the MOW after it outflows through the Strait of Gibraltar, while Formigas, located further away in the middle of the Atlantic, is influenced by the westward branch of the MOW (Bashmachnikov et al., 2015).

The Gazul mud volcano is located in the continental slope of the Gulf of Cadiz (Palomino et al., 2015). Gazul is sculpted by the MOW, which has carved two downstream depressions at both sides of the structure, whereas its rear sector has a peculiar saddle shape as result of the low velocities that enable sedimentation (Rueda et al., 2012; Palomino et al., 2016). The Ormonde seamount forms part of the Gorringe Bank at around 125–150 miles west-southwest of Cape St. Vincent. It presents a steep southeastern flank with gullies and incipient canyons and a northwestern flank without remarkable incised features. At the southwestern, it is separated of the Gettysburg seamount by a passage of a maximum depth of 800 m. The Formigas seamount is at the southeastern part of the Azores. Its western section is occupied by a 1,800 m depth flat abyssal plain, with a few of incipient gullies, and at the northeastern side, around twenty knolls are spread on an area of 130 km^2.

Data

In order to characterize hydrographically and dynamically the Gazul mud volcano and the Ormonde and Formigas seamounts, both climatological and *in situ* field data were used. The climatological data include mean annual temperature, near-surface current velocities, mean winds and Sea Surface Temperature. The mean annual temperature was obtained from the Roemmich-Gilson Argo Climatology, generated using Argo temperature and salinity data interpolated with a weighted

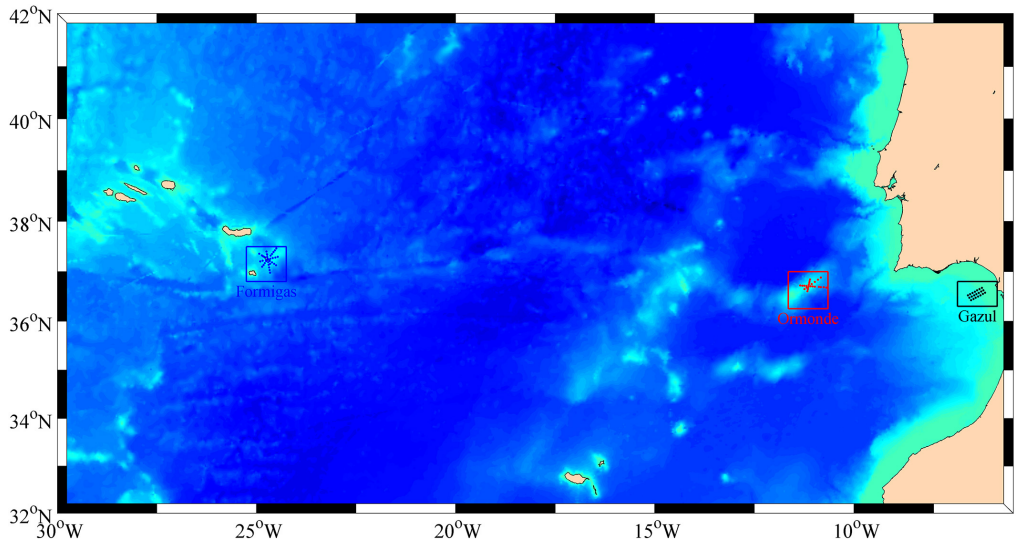

FIGURE 1 | Distribution of the stations for the three regions of the MEDWAVES Atlas Cruise contemplated in this study: the Formigas (in blue) and Ormonde (in red) seamounts, and the Gazul mud volcano (in black).

least-squares fit, as described in Roemmich and Gilson (2009). The near-surface current velocities were derived by the NOAA Atlantic Oceanographic and Meteorological Laboratory using observations from surface drifting buoy observations (Lumpkin and Johnson, 2013), and the mean wind and Sea Surface Temperature data were produced by the NOAA Earth System Research Laboratory. Sea Surface Temperature was obtained from the daily High-Resolution-Blended satellite Analyses product (Reynolds et al., 2007). The mean wind, interpolated using a wide range of observing systems, was obtained from the International Comprehensive Ocean-Atmosphere Data (ICOADS). A more detailed description of the datasets used can be found in **Table 1**.

Data from the TPXO7.2 model was used to describe the barotropic tidal regime in each of the regions of study. This model uses a generalized inverse method, which assimilates altimeter data to predict tide height and currents (Egbert and Erofeeva, 2002).

The *in situ* field data were gathered during the MEDWAVES cruise carried out between the 21st of September and the 25th of October 2016, on board the RV Sarmiento de Gamboa, as part of the H2020 ATLAS Project. In each of the three features (**Figure 1**) a specifically designated sampling grid was carried out. In the Gazul mud volcano, located in the continental slope of the Gulf of Cadiz, three hydrographic sections, perpendicular to the flow, were carried out, with 21 hydrographic stations in total. In the Ormonde seamount, which is part of the Gorringe Bank, 25 hydrographic stations were carried out in a radial grid perpendicular to the bathymetry. In the Formigas seamount, southeastern of the Azores, 41 hydrographic stations were carried out in a radial grid perpendicular to the bathymetry.

In each station, conductivity, temperature, oxygen concentration, and pressure were measured with redundant temperature and salinity sensors from a Seabird 9111 CTD. Additionally, at each hydrographic station, velocity data were acquired from a Lowered Acoustic Doppler Current Profilers (LADCP) system composed of a dual 300 kHz LADCP. The LADCP data were processed according to Fischer and Visbeck (1993). LADCP data were used to estimate the velocity in the assumed layer of no-motion by comparing the LADCP with the geostrophic velocity profile at each station as indicated in Comas-Rodríguez et al. (2010). The data were acquired at each station from the surface down to 10 m above the bottom. Distance intervals between stations were approximately 5 km to resolve mesoscale. Temperature and pressure sensors were calibrated at the SeaBird laboratory before the cruise. On board salinity calibration was carried out with a Guildline Autosal model 8400B salinometer with a precision better than 0.002 for single samples.

In addition, a total of 17 video transects were also recorded in the three target features using the ROV Liropus. Positioning of the ROV was achieved using the HYPACK software. The ROV was equipped with a HD color zoom video camera illuminated by Sealite Spheres, an underwater photo still camera and a pair of parallel laser pointers mounted 10 cm apart (see specifications in Orejas et al., 2017). A set of geo-referenced still images extracted from the ROV video transects at 5 m intervals was used to characterize the benthic communities. To allow comparison between the different features, only those images within 1.5–2.5 m width range were retained for analyses. Low quality images that prevented from fauna identification were also excluded. Benthic organisms larger than 5 cm were identified to the lowest possible taxonomic level and the abundances were aggregated for total invertebrates and the phyla Porifera and Cnidaria. The Formigas seamount is the largest of the studied features, hence surrounded by several water masses, and also covers a large depth range (from 500 to 1,500 m depth). That makes this feature the most suitable one to study the influence of different water

TABLE 1 | Climatological data.

Data	**Argo temperature climatology**
Source	Scripps Institution of Oceanography: http://sio-argo.ucsd.edu/RG_Climatology.html
Time period	From 2004 to 2014
Spatial coverage	1/6 × 1/6 degree
Measurements	Mean temperature (degree Celsius)
References	Roemmich and Gilson, 2009
Data	**Annual means of drifter data**
Source	NOAA/AOML and NOAA/PMEL: http://www.aoml.noaa.gov/phod/dac/dac_meanvel.php
Time period	From 1979 to 2015
Spatial coverage	1/2 × 1/2 degree
Measurements	Zonal and meridional current velocity coefficients (m/s)
References	Lumpkin and Johnson, 2013
Data	**Climatological monthly means of drifter data**
Source	NOAA/AOML and NOAA/PMEL: http://www.aoml.noaa.gov/phod/dac/dac_meanvel.php
Time period	From 1979 to 2015
Spatial coverage	1/2 × 1/2 degree
Measurements	Zonal and meridional current velocities (m/s)
References	Lumpkin and Johnson, 2013
Data	**NOAA High Resolution SST Data**
Source	NOAA/OAR/ESRL PSD: http://www.esrl.noaa.gov/psd/
Time period	From 1981 to 2017
Spatial coverage	1/4 × 1/4 degree
Measurements	Daily mean Sea Surface Temperature (degree Celsius)
References	Reynolds et al., 2007
Data	**ICOADS 1-degree enhanced**
Source	NOAA/OAR/ESRL PSD: http://www.esrl.noaa.gov/psd/
Time period	From 1960 to 2014
Spatial coverage	1 × 1 degree
Measurements	Zonal and meridional wind monthly mean at surface (m/s)
References	ICOADS website publications page: http://icoads.noaa.gov/publications.html

masses in the presence of benthic communities dominated by suspension feeders. From seven video transects conducted in the Formigas seamount, a total of 801 images were analyzed. Abundances for the whole invertebrate community (including five phyla), porifera and cnidarians were averaged in 2 m bins along the depth gradient of Formigas seamount.

RESULTS

Overview

All the study targets are located in the area of influence of the east side of the North Atlantic Subtropical Gyre. The surface temperatures in this area decrease northward (**Figure 2**), reaching annual mean temperatures between 18 and 20°C. At the latitudes of the sampled features, between 38 and 36°N, the temperature also decreases toward mainland; with a temperature difference of around 1°C between Formigas and Gazul (**Figure 2**). This temperature difference is the result of the near-surface currents governing in this area: the Azores Current and the branch it splits near Madeira, which meanders toward the Strait of Gibraltar (Johnson and Stevens, 2000; Sala et al., 2016), prone to form cyclonic meanders at its north side and anticyclonic ones at the south (Juliano and Alves, 2007), and the Portugal Current, which flows southwards along the Iberian shelf (**Figure 3**), until it reaches the Azores Current, which acts as boundary between the north and south circulation of the North Atlantic Subtropical Gyre (Relvas et al., 2007).

These near-surface currents are not constant all year round and in fact they show strong seasonal variability (**Figure 3**). Thus, in winter (**Figure 3A**), the eastward branch of the Azores Current (34°N) is intense and well defined, flowing directly to the Strait of Gibraltar. In autumn (**Figure 3D**), the Azores current is still observed, although weaker. However, during both, spring and summer (**Figures 3B,C**), the surface current flowing to the east at the surface, almost disappears, and it turns southward, toward the Canary Current, due to the intensification of the trade winds during those seasons. Similarly, there is a shift in the currents north of the Azores. In winter and autumn (**Figures 3A,D**), the current flows eastwards, while in spring and most of the summer (**Figures 3B,C**) there is a southward flow perpendicular to the islands (25°W). The Azores islands, islets and seamounts act as a barrier that weaken the flow and alter its course; hence the current barely reaches the area surrounding the Formigas seamount.

In the Ormonde area, the Portugal Current flows over the seamount all year long. Although, it can be observed a slight decrease in intensity as the flow goes between the seamounts. In general, this current gets weaker as it goes south. The Portugal Current is stronger in summer, remaining considerably constant for the rest of the year, and it produces a cyclonic gyre in winter and, to a lesser extent, in autumn, when it reaches the eastward Azores Current.

In the region where the Gazul mud volcano is located, there is a strong current to the south-southeast that eventually goes through the Strait of Gibraltar. During the months of winter and autumn, this flow is also fed by the Azores Current. However, as this current does not reach the Gulf of Cadiz in spring and summer, the additional input of water is smaller and comes from the Portugal Current.

Similar seasonal patterns were found in the monthly mean winds. In Formigas (**Figure 4A**) the winds vary both in intensity and direction. During the winter months, the winds are predominantly from the southwest, while in summer the north component is more important and the winds are also more intense. In Ormonde (**Figure 4B**) the winds do not change much in direction, but they do change in intensity, with maximums in July. Finally, in Gazul (**Figure 4**) the winds are also more intense in summer, and they shift from northeast in winter to northwest in summer. The variation of the winds also affects the sea surface temperature. It seems very similar in the three areas, with a minimum of temperature around March, and a maximum that shifts from September–October in Formigas and Ormonde (**Figures 4D,E**) to August–September in Gazul (**Figure 4F**).

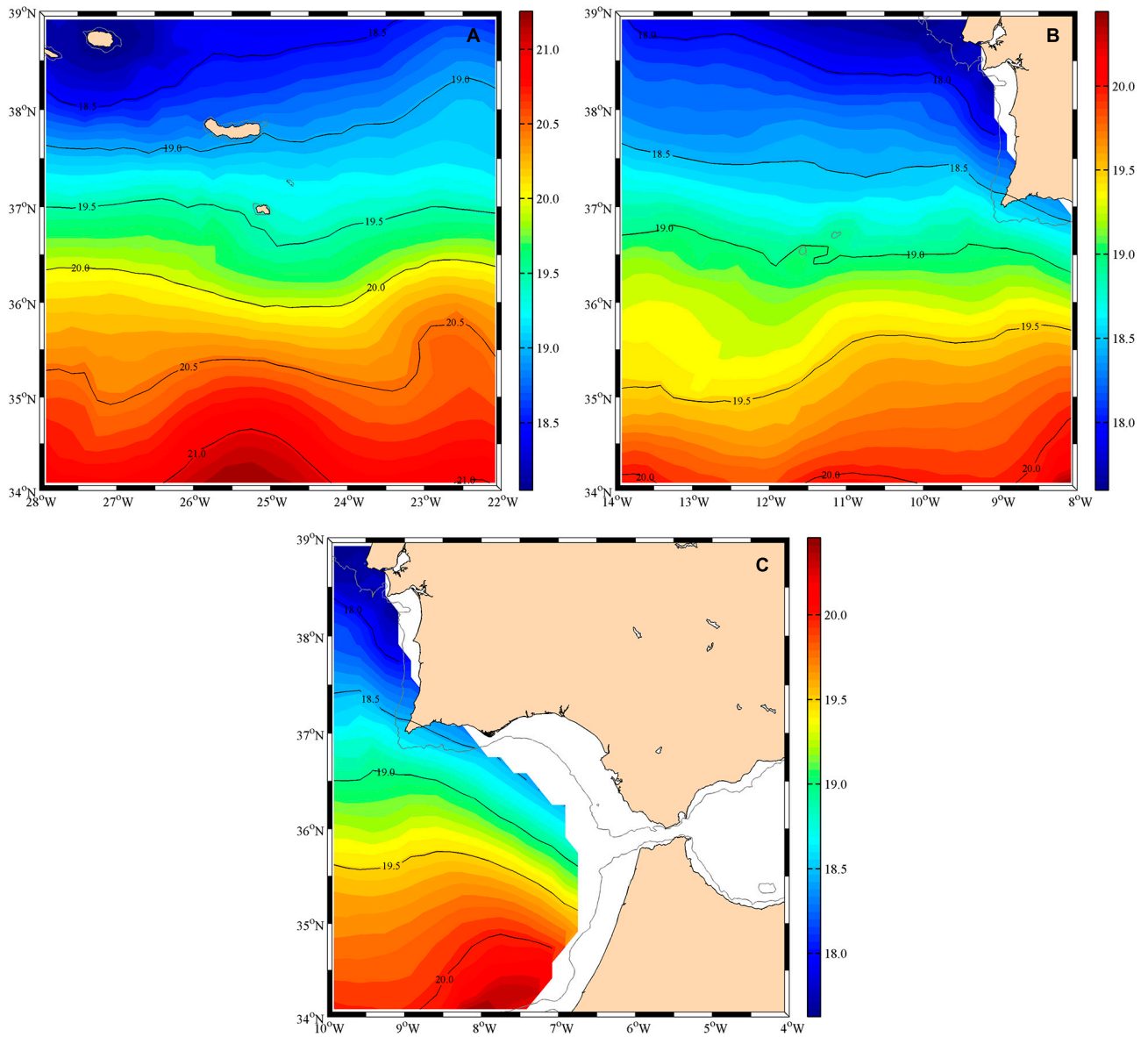

FIGURE 2 | Mean annual temperature in degrees Celsius in the Formigas **(A)** and Ormonde **(B)** seamounts, and the Gazul mud volcano **(C)**.

However, the temperature is around 1°C lower in Ormonde, with values between 15°C and 22°C, than in Formigas and Gazul, both in winter and in summer. This is probably consequence of the strong north-northwest winds present in the Ormonde region all year round.

In summary, the mean ocean circulation in the region of study is subject to high seasonal variability, and therefore do not provide permanent favorable conditions for the development of Taylor caps, which require a unidirectional steady current to be formed (Lavelle and Mohn, 2010). However, in spite of the unsteadiness, Taylor caps could still be generated (Beckmann and Mohn, 2002). In order to identify the hydrodynamical phenomena governing the circulation over the these underwater features in the path of the MOW, and, in particular, to verify if Taylor caps are formed, we will analyze, in the next section, the regional dynamics over the three features.

Dynamics

As it was pointed out in the previous section, the mean ocean over the three underwater features in the pathway of the MOW does not meet the conditions for the formation of Taylor caps. To evaluate whether, in spite of the unsteadiness, Taylor caps could still be generated, in this section, we will describe the dynamics over the Ormonde and Formigas seamounts and the Gazul mud volcano found during the MEDWAVES cruise.

In the Gazul mud volcano the upper ocean circulation is characterized by a two-layer flow, with the lighter North Atlantic Central Water (NACW) on top of the heavier MOW, as it can

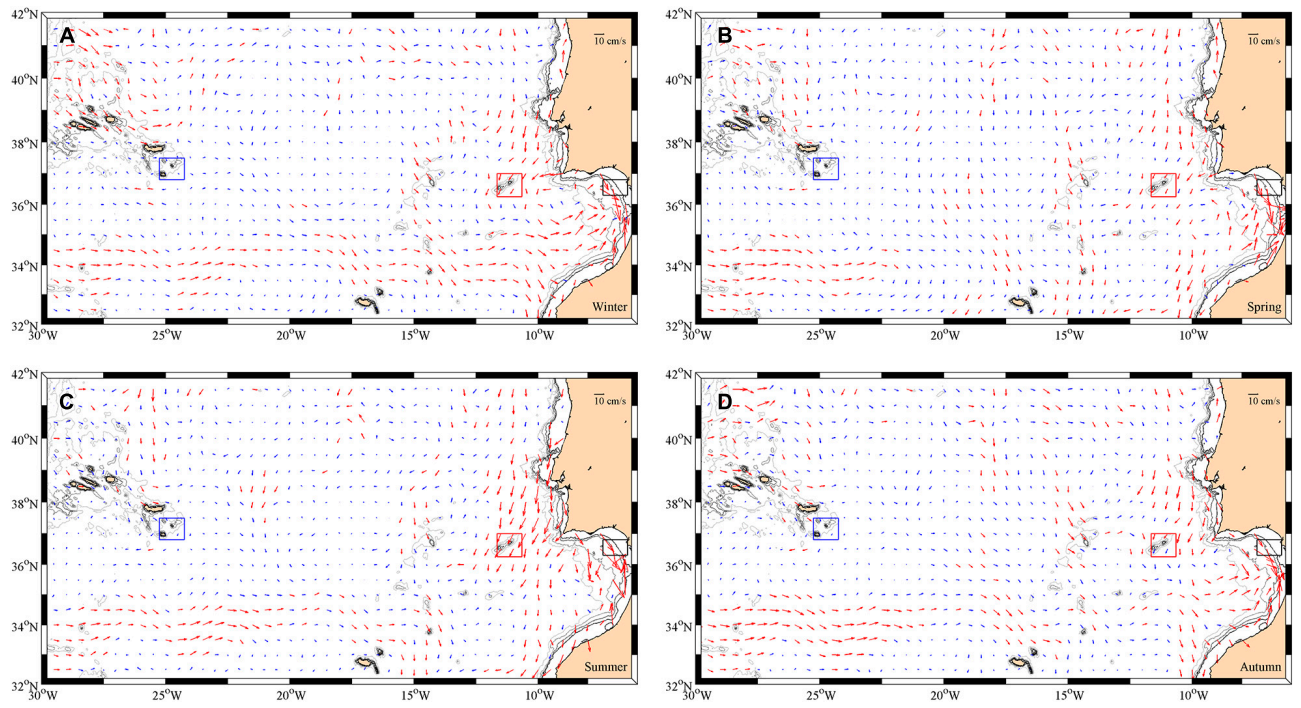

FIGURE 3 | Seasonal near-surface current velocities. The blue arrows correspond to velocity values under 5 cm/s and the red arrows to values from 5 to 40 cm/s. The squares are the areas of study: the Formigas (in blue) and Ormonde (in red) seamounts, and the Gazul mud volcano (in black). Each panel corresponds to a different season: **(A)** winter, **(B)** spring, **(C)** summer, and **(D)** autumn.

be observed in the horizontal distribution of LADCP velocities (**Figure 5**). The upper layer (**Figure 5A**) flows eastward along the first 400 m of all the region of Gazul, transporting the Atlantic waters into the Strait of Gibraltar. On the other hand, the MOW exits through the Strait close to the bottom (**Figure 5B**). This deep outflow moves westward close to the slope of the Gulf of Cadiz. It is interesting to notice the disruption of the current on its path close to 36°30′N 6°90′W, which turns the flow to the north at both the upper and the deeper level.

Over the Ormonde seamount, the strong influence of the Azores Current lead the predominant flow to the east, as it is shown in the horizontal distribution of velocities (**Figure 6**). Thus, between the 40 and 540 m (**Figure 6A**), there is a strong eastward current; however, in the intermediate layer (560–1,000 m) (**Figure 6B**) the seamount disrupts the flow. This disruption causes a constant flow around the southwest part of the seamount, resulting in a weak anticyclonic circulation around Ormonde.

The circulation in the Formigas area does not follow a well-defined pattern (**Figure 7**), since the presence of the seamount and the islets greatly disrupts the flow. In the top 800 m (**Figures 7A,B**) the flow is deflected to the northeast, while at the intermediate layer (560–1,000 m) the flow is diverted, surrounding both flanks of the seamount. At greater depths, the northern branch of the flow is blocked by the San Miguel Island, and the main flow surrounds the Formigas seamount by its south flanks, describing a weak anticyclonic circulation.

The analysis of the barotropic tidal regime shows a different behavior in each of the areas studied. For the Gazul mud volcano the tide has velocities of about 2 cm/s in the northeast-southwest direction (**Figure 5A**). However, in both the Ormonde (**Figure 6A**) and Formigas (**Figure 7A**) seamounts the tides are stronger, reaching the 5 cm/s, but in opposite directions, with a northwest-southeast tide for Ormonde and a northeast-southwest one for Formigas.

Hydrography

The Mediterranean water, after outflowing through the Strait of Gibraltar flows westward over the Gazul mud volcano. After that, the MOW continues its spread into the Atlantic, reaching the Ormonde seamount, which diverts the flow toward the southwest, forcing it to surround the seamount, and finally it reaches Formigas.

Hence, the three regions are characterized by the presence of the MOW at mid-depths. In fact the θ/S diagrams (**Figure 8**) for the areas sampled show a similar vertical distribution of water masses. In particular, all of them have a relative salinity minimum around γ^n 27.160 kg/m^3, indicative of the presence of the NACW, and a relative maximum of salinity at γ^n 27.630 kg/m^3, distinctive feature of the MOW. This maximum shows an intensity decrease from Gazul to Formigas which characterizes the propagation of the MOW into the Atlantic.

Specifically, the Gazul mud volcano (**Figures 9A–C**) shows a vertical distribution divided in three layers. In the first 10–20 m there is a mixed layer in which the temperature

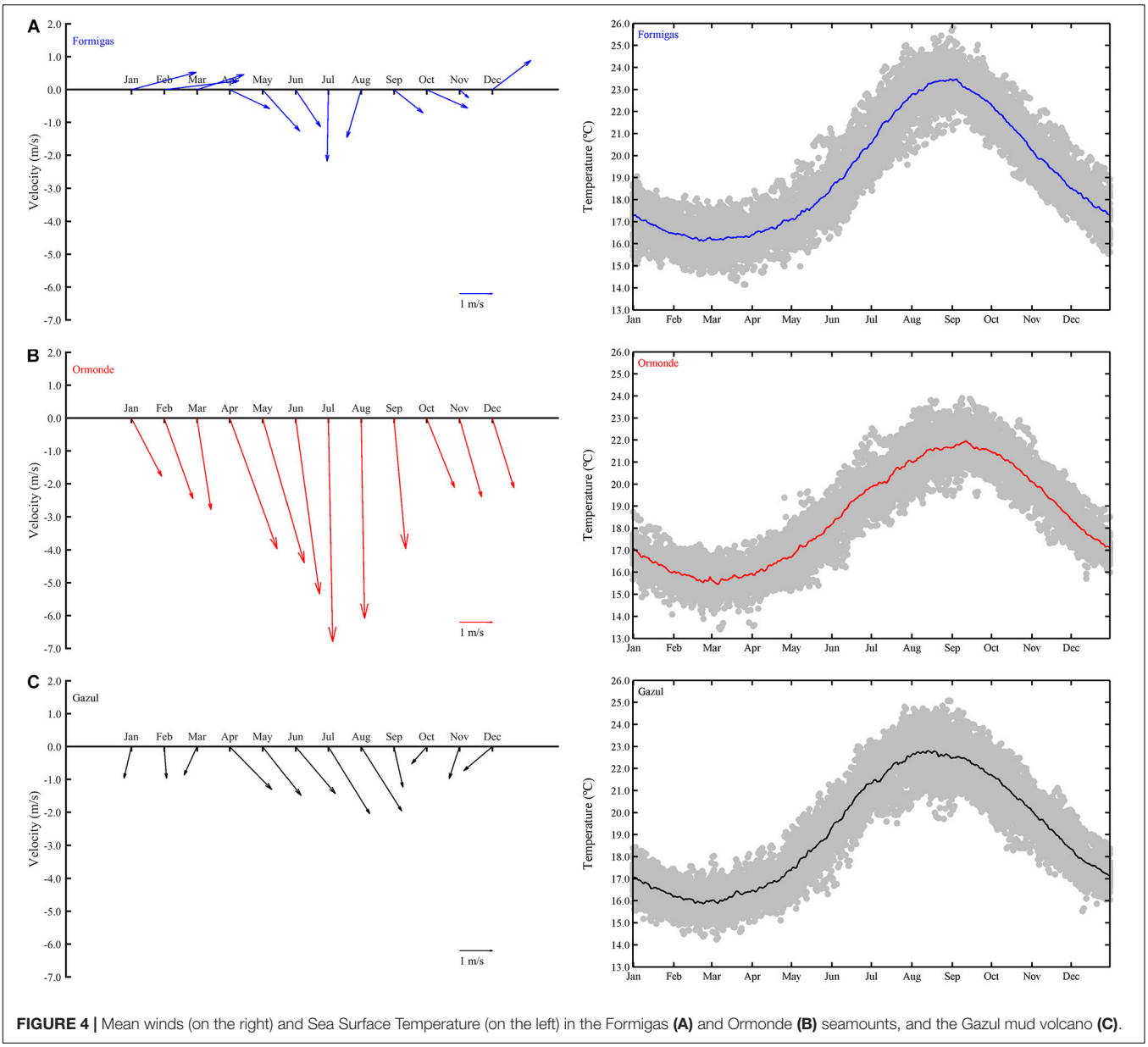

FIGURE 4 | Mean winds (on the right) and Sea Surface Temperature (on the left) in the Formigas **(A)** and Ormonde **(B)** seamounts, and the Gazul mud volcano **(C)**.

and the salinity are almost constant, followed by the seasonal thermocline that reaches 50 m in the stations located away from the coast. Just below the surface layer, it is located the NACW, which is characterized by an almost linear relationship between temperature and salinity, reaching its minimum (11.87°C and 35.67) between 300 and 450 m. Finally, separated from the NACW, by the isohaline of 35.75 and the 27.162 kg/m^3 isopycnal (and the 12.50°C isotherm), the MOW occupies approximately the deepest 150 m from the bottom. In this layer, there is an increment in both temperature and salinity, with maximum values of 36.57 and 13.64°C, and a relative minimum in the oxygen concentration (**Figure 9D**).

Regarding the Ormonde seamount (**Figures 10A–C**), the surface layer is located above the isopycnal of 26.850 kg/m^3, and the surface waters are divided among a mixed layer that goes down almost 50 m and the seasonal thermocline, reaching depths less than 100 m. Between the 100 and 400 m (isopycnals of 26.850 and 27.200 kg/m^3), the NACW shows its characteristic linear decrease of temperature and salinity. Below the NACW, and between the 27.380 and 27.820 kg/m^3 isopycnals, there is a sharp increase in salinity consequence of the presence of the MOW. The temperature is practically constant, with a small increase until 900 m, where it reaches a relative maximum of 12°C. However, the increase of salinity continues until depths of 1,200 m, with values up to 36.44. There is a second core around the 800 m, near the 27.620 kg/m^3 isopycnal, where a less noticeable maximum of salinity can be found. The influence of the MOW is noticeable from 500 to 1,400 m, with values of oxygen concentration reaching the characteristic

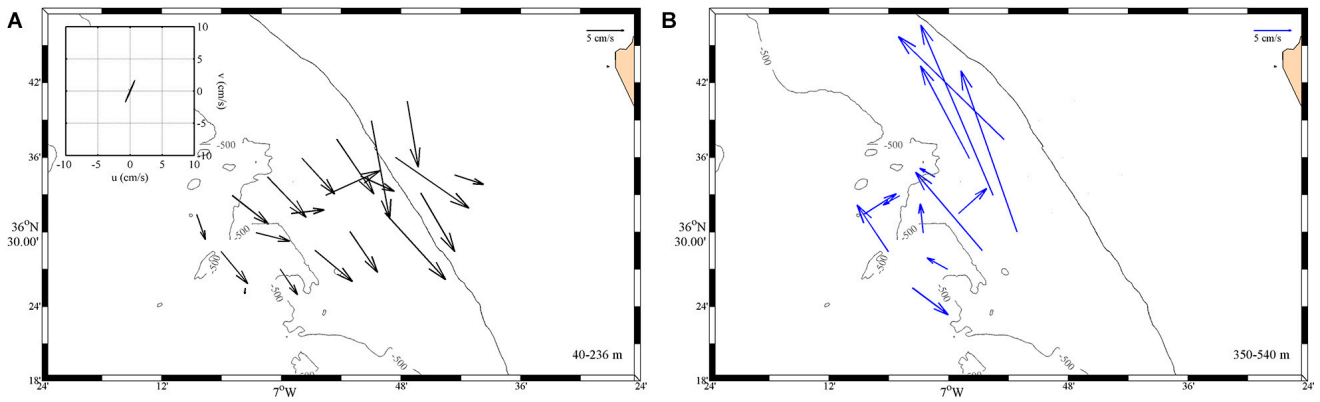

FIGURE 5 | Horizontal distribution of vertically averaged Lowered Acoustic Doppler Current Profilers (LADCP) velocities for the Gazul mud volcano. The figure on the left **(A)** corresponds to the upper layer (40–236 m) and the figure on the right **(B)** to the deep layer (350–540 m). The tidal ellipses in the average location of Gazul are included on the inset in the top left corner of panel **(A)**, with the same scale as the main plot.

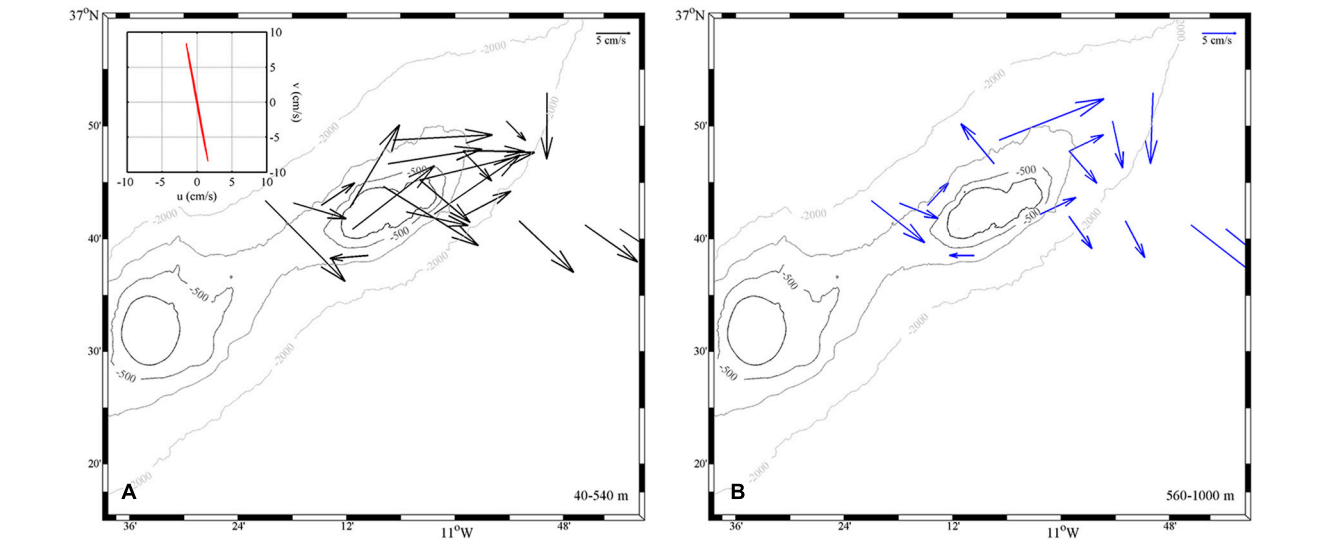

FIGURE 6 | Horizontal distribution of vertically averaged LADCP velocities for the Ormonde seamount. The figure on the left **(A)** corresponds to the upper layer (40–540 m) and the figure on the right **(B)** to the deep layer (560–1000 m). The tidal ellipses in the average location of Ormonde are included on the inset in the top left corner of panel **(A)**, with the same scale as the main plot.

minimum of the Mediterranean waters (**Figure 10D**). Below the MOW there is a rapid decrease of temperature and salinity that indicates the presence of the upper North Atlantic Deep Waters (uNADW).

In the case of Formigas, the first 100 m of the water column (**Figures 11A–C**) are occupied by a mixed layer of about 20–30 m and the seasonal thermocline. Below, the NACW, delimited by the 26.850 kg/m^3 and the 27.200 kg/m^3 isopycnals (150–600 m), shows a decrease of temperature from 14.57 to 11.58°C and of salinity from 35.94 to 35.60. Below the NACW the salinity continues to decrease slightly reaching a minimum value of 35.56 at 675 m. This indicates the presence of Antarctic Intermediate Waters (AAIW), due to the location of the seamount in the surrounding area of the Atlantic Ridge. Under the AAIW, the MOW in Formigas shows an increment of salinity, although less pronounced than in the other two regions, as a result of the dilution that the MOW undergoes during its path from the Strait of Gibraltar. Thus, this diluted MOW, between γ^n of 27.380 and 27.720 kg/m^3, shows a maximum of salinity of 35.81 close to 900 m. The minimum of oxygen concentration (**Figure 11D**) are, in the case of Formigas, practically restricted to the core region, and it does not reach values as low as in Ormonde. The influence of the Mediterranean waters reaches almost the 1,400 m, until the 35.25 isohaline and the 27.820 kg/m^3 isopycnal. The layer close to the bottom is occupied by the uNADW that is characterized by decreasing values of salinity and temperature.

The study of the distribution of water masses shows the characteristic spread of the MOW in the Atlantic. The decrease of salinity from Gazul to Formigas denotes the westward flow of this water mass. The low salinity values present in Formigas are result

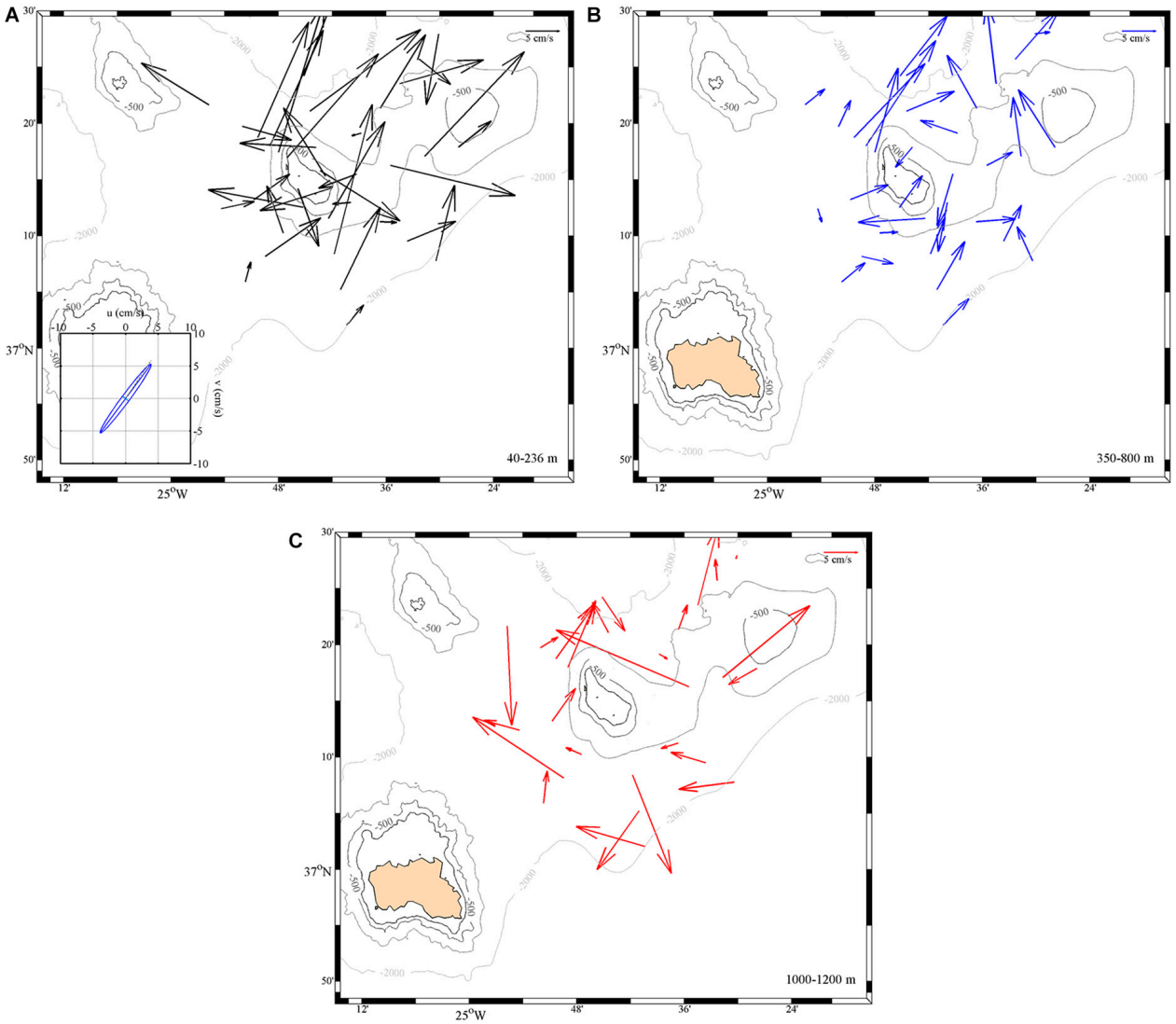

FIGURE 7 | Horizontal distribution of vertically averaged LADCP velocities for the Formigas seamount. The upper figure on the left **(A)** corresponds to the upper layer (40–236 m), the upper figure on the right **(B)** to the intermediate layer (350–800 m) and the bottom figure **(C)** to the upper deep waters (1000–1200 m). The tidal ellipses in the average location of Formigas are included on the inset in the top left corner of panel **(A)**, with the same scale as the main plot.

of the long distance of this seamount with the source. Besides, the depth at which the core is found changes among the regions. In Gazul the MOW occupies the bottom layer, but it gets deeper at Ormonde, where two cores were found. Finally, a more diluted MOW arrives at Formigas. However, in Formigas it can just be described a single not conspicuous core at a depth between the cores in Ormonde.

As a consequence of the presence of the MOW, there are areas below the permanent thermocline, where the Brunt–Väisälä frequency reaches maximum values. In Gazul (**Figure 9E**), two relative maxima are found: the first one, from surface to the upper limit of the NACW, in the area of the seasonal thermocline, and the second one in the boundary between the NACW and the MOW, where an intense halocline occurs. High values are also found near the bottom, close to the core of the MOW. In Ormonde (**Figure 10E**), the maximum Brunt–Väisälä values are in the area of the thermocline. However, relatively high values are also found in the MOW layer, mainly in the limit with the NACW and related with the subsurface salinity maxima. Similarly to what was found in Ormonde, in Formigas (**Figure 11E**) the maximum values of the Brunt–Väisälä frequency occur in the surface, although there is a subsurface maximum in the upper limit of the MOW, related with the relative maximum of salinity.

Thus, these relatively high values of the Brunt–Väisälä frequency, due to the salinity difference produced by the MOW, generate a strong density gradient mainly in the NACW–MOW interface. According to numerical models a mid-water intense stratification layer can boost the internal waves in its particular depth range when interacting with certain slope values

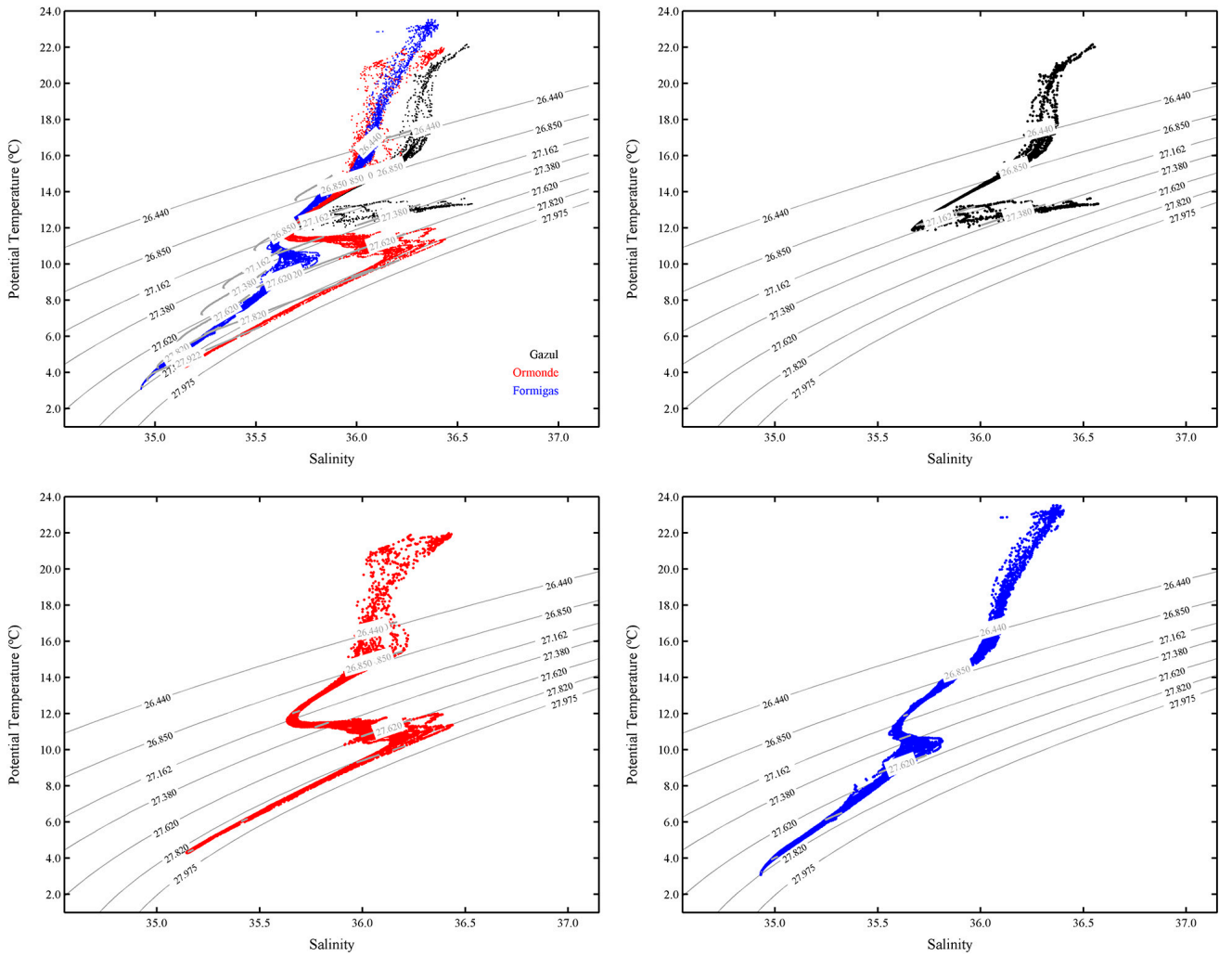

FIGURE 8 | θ/S diagrams of all the stations sampled during the MEDWAVES cruise in the Gazul mud volcano (in black), and the Ormonde (in red), and Formigas (in blue) seamounts. The thin gray lines correspond to the density isolines, while the thick gray lines correspond to the neutral density isopycnals.

resulting in local relatively strong currents (Hall et al., 2013). The characteristic slope of these internal waves (c) will be dependent of the Brunt–Väisälä frequency and it is given by:

$$c = \pm\sqrt{\frac{\omega^2 - f^2}{N^2 - \omega^2}}$$

where ω is the wave frequency (in this study the frequency of the semidiurnal tide was used), f is the Coriolis parameter, and N is the Brunt–Väisälä frequency.

The relationship between this angle and the slope of the bottom (γ) will determine the behavior of the internal waves as determined by Cacchione and Wunsch (1974). If $\gamma/c < 1$, the slope is subcritical, and the waves will be transmitted; if $\gamma/c \approx 1$, the slope is critical, and the waves will break; if $\gamma/c > 1$, the slope is supercritical, and the waves will be reflected.

In the Gazul mud volcano (**Figure 12A**) the ratio γ/c goes from subcritical to critical or even supercritical where there is a sudden change in depth, while the steep slope of the Ormonde and Formigas (**Figures 12B,C**) seamounts supports mainly supercritical behaviors, which causes the reflection of internal waves preventing them to break. However, in the areas where the ratio γ/c is critical (**Figure 12**) internal waves will break, producing turbulence.

In addition, at the latitude of the regions of study, poleward 30°N, the local inertial period ($2\pi/f$) is longer that the tide oscillation period and the internal waves can be trapped at the slopes of the seamounts. This trapping may generate a residual current along the slope that can be amplified, with the largest amplification expected at a bottom depth where $N * \sin(\alpha)$ reaches a maximum value being α the inclination of the seabed [i.e., $\alpha = \tan^{-1}(\gamma)$] (Huthnance, 1981).

The depth of the maximum amplification (**Figure 13C**) coincides with the areas of high values of N (**Figure 13B**), modulated by the step topography of those underwater features (**Figure 13A**). In particular, Gazul shows a maximum at the

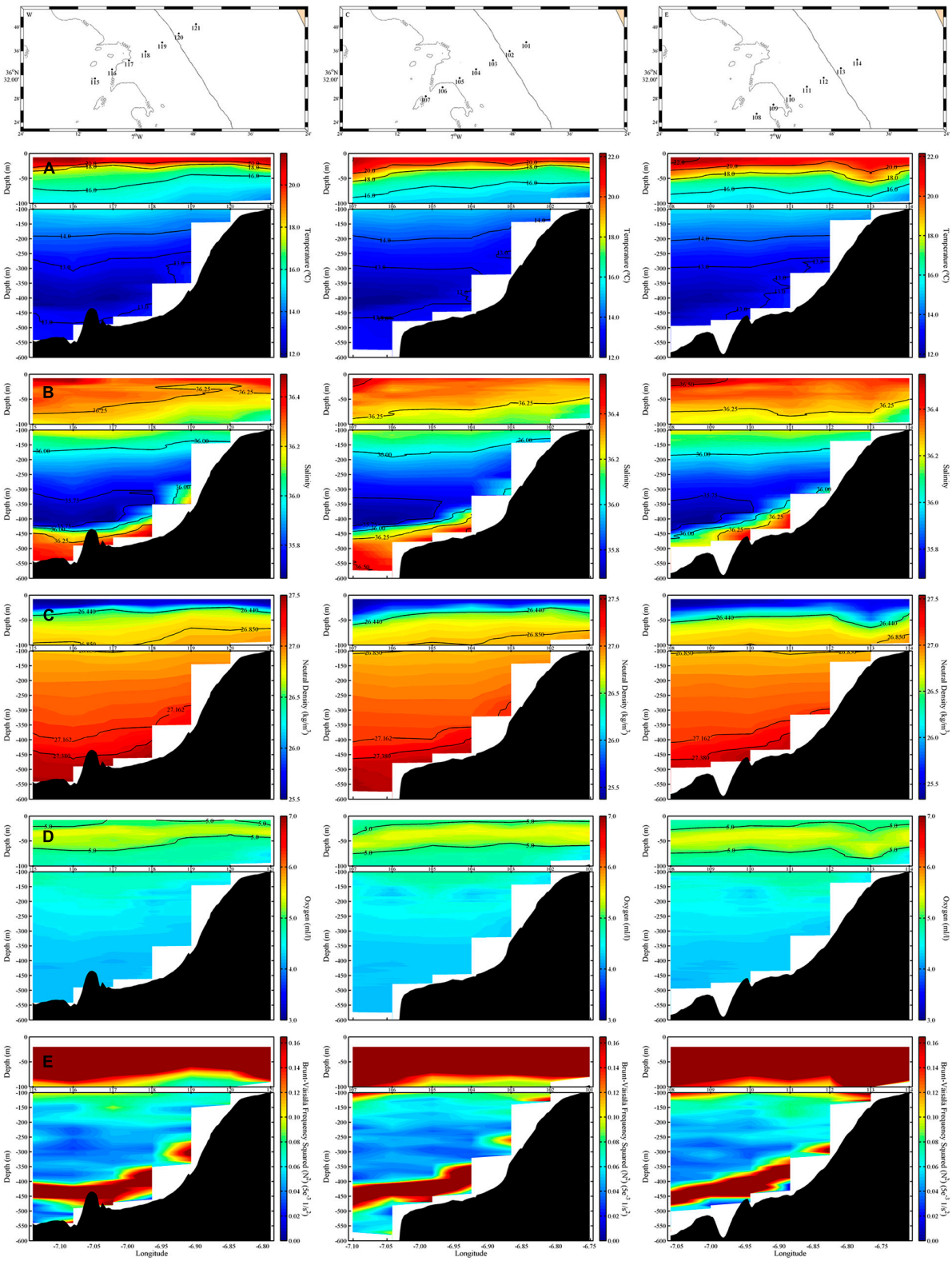

FIGURE 9 | Vertical sections of (from top to bottom) potential temperature (°C) **(A)**, salinity **(B)**, neutral density (kg/m^3) **(C)**, oxygen concentration (ml/l) **(D)**, and Brunt–Väisälä frequency squared (5e^{-3} 1/s^2) **(E)** in the Gazul mud volcano. For each one of the vertical sections, the upper panel corresponds to the top 100 meters, while the lower panel corresponds to the 100–600 meters depth range. The numbers between both panels correspond to the station numbers, which are localized in the corresponding map at the top.

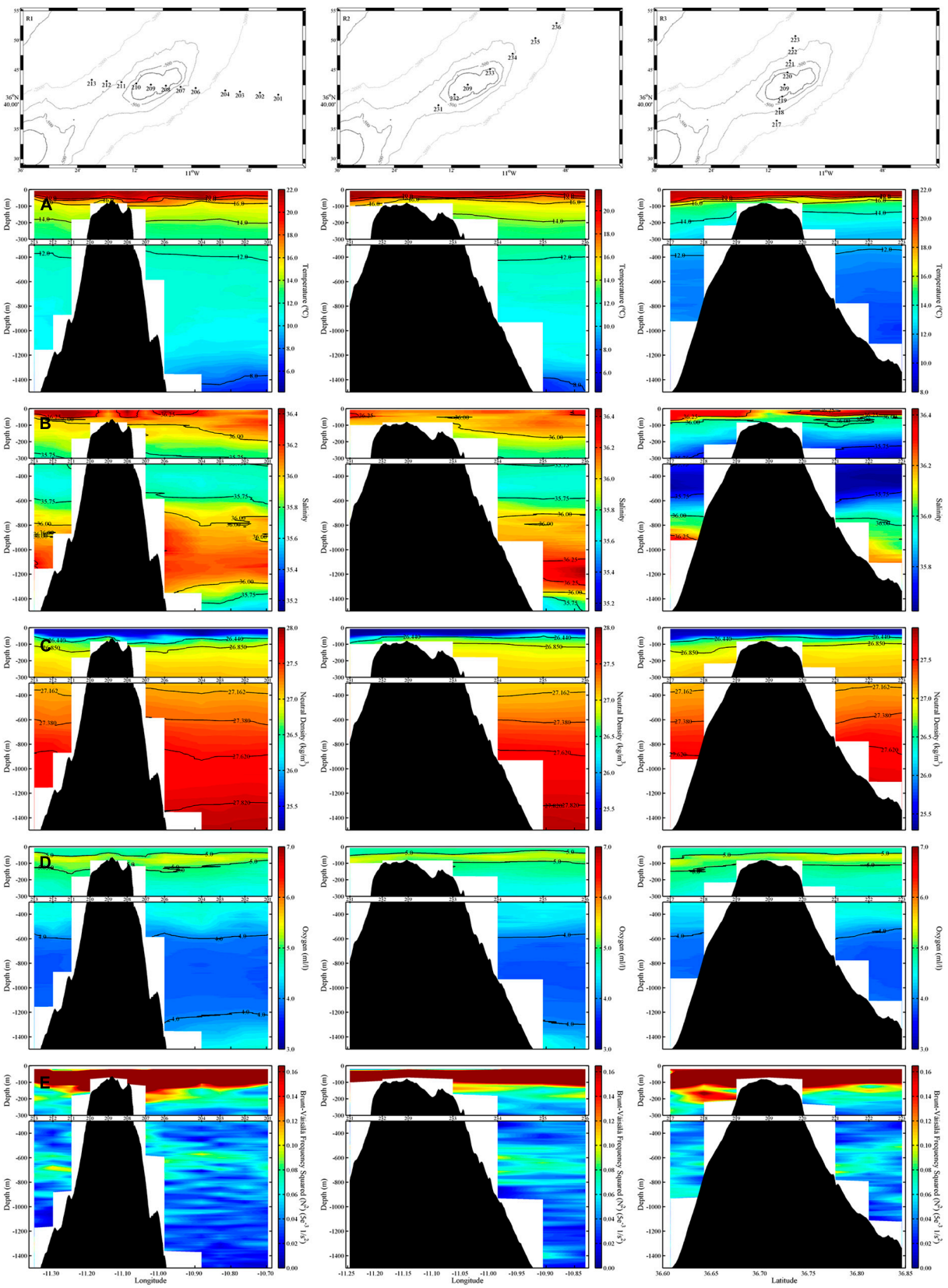

FIGURE 10 | Same as **Figure 9**, but for the Ormonde seamount.

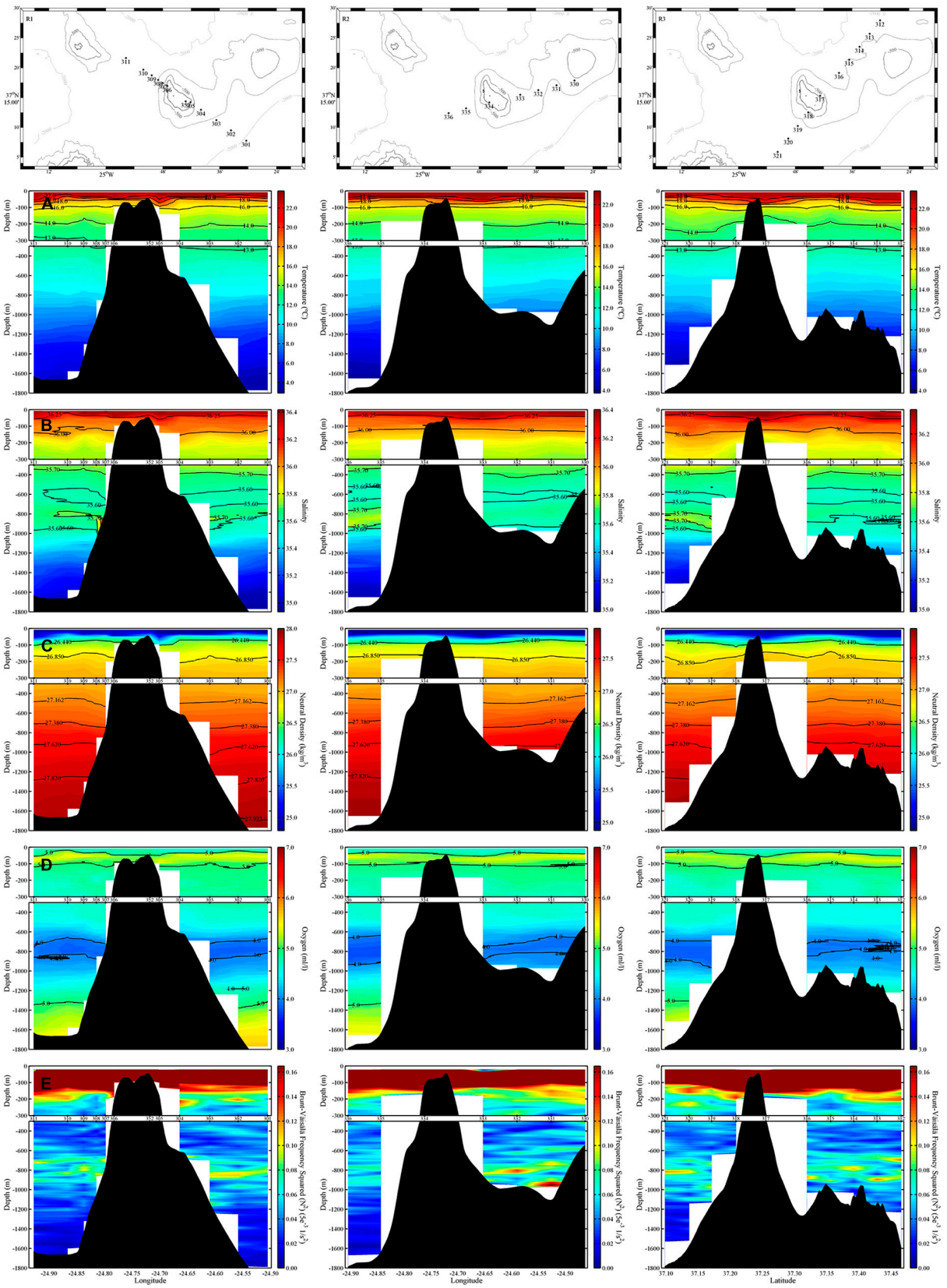

FIGURE 11 | Same as **Figure 9**, but for the Formigas seamount.

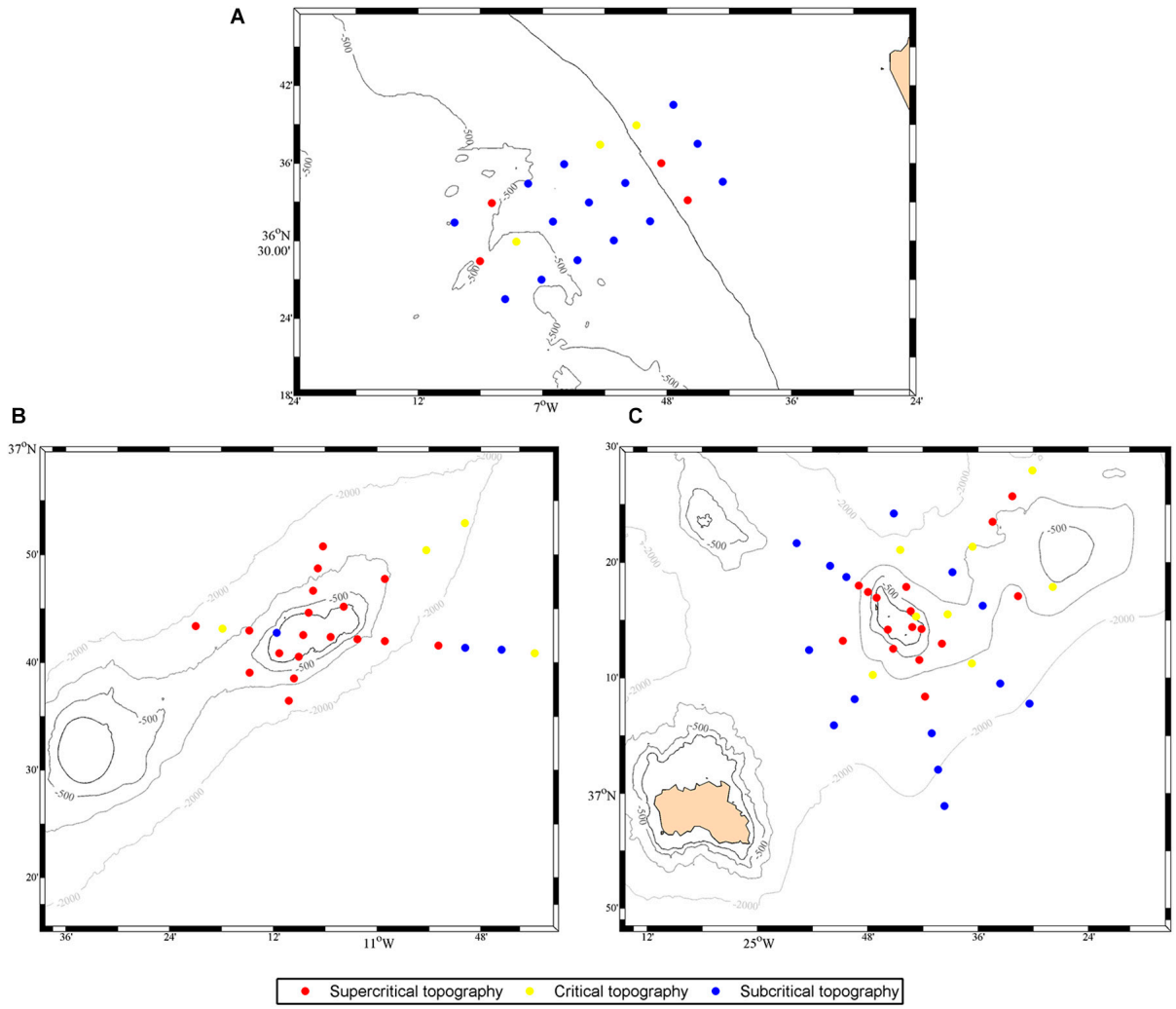

FIGURE 12 | Bottom slope (γ) vs. angle of propagation of internal waves (c) near the bottom for the Gazul mud volcano **(A)**, the Ormonde **(B)**, and Formigas **(C)** seamounts.

NACW–MOW interface. The same maximum can be found in Ormonde, together with a second one at the MOW–NADW interface. The case of Formigas is slightly different, since the presence of a third water mass, the AAIW, between the NACW and the MOW generates a region of maximum amplification from the low boundary of the NACW until the core of the MOW, not showing another significant maximum below the 1,000 m.

Benthic Communities

A total of 9729 megabenthic invertebrates belonging to 5 different phyla (Porifera, Cnidaria, Arthropoda, Echinodermata, and Bryozoa) were identified in the still images, which included 3684 poriferans and 5736 cnidarians (37.87 and 58.96% of the total abundance registered). The average number of organisms of each group was displayed along the depth gradient of the Formigas seamount. The highest number of benthic organisms occurred between 500 and 1,000 m depth, coinciding with the NACW–MOW interface (**Figure 14A**). The same pattern was also observed for porifera and cnidaria (**Figures 14B,C**).

SUMMARY AND DISCUSSION

As indicated by Lavelle and Mohn (2010), the formation of Taylor caps would generate an anticyclonic gyre that isolates the flow on the top of the seamount. However, although the circulation in the three regions of study is disrupted by the presence of the underwater features, the circulation associated with Taylor caps was not observed. Theoretically, the isolation produced by a Taylor cap on the top of a seamount will enhance the productivity in the area. However, the importance of this phenomenon and the likelihood with which it occurs in the field may be uncertain, since flows in the ocean are not usually steady (Lavelle and Mohn, 2010). The dynamical analysis of three features in the path of the MOW does not show any evidence of Taylor caps

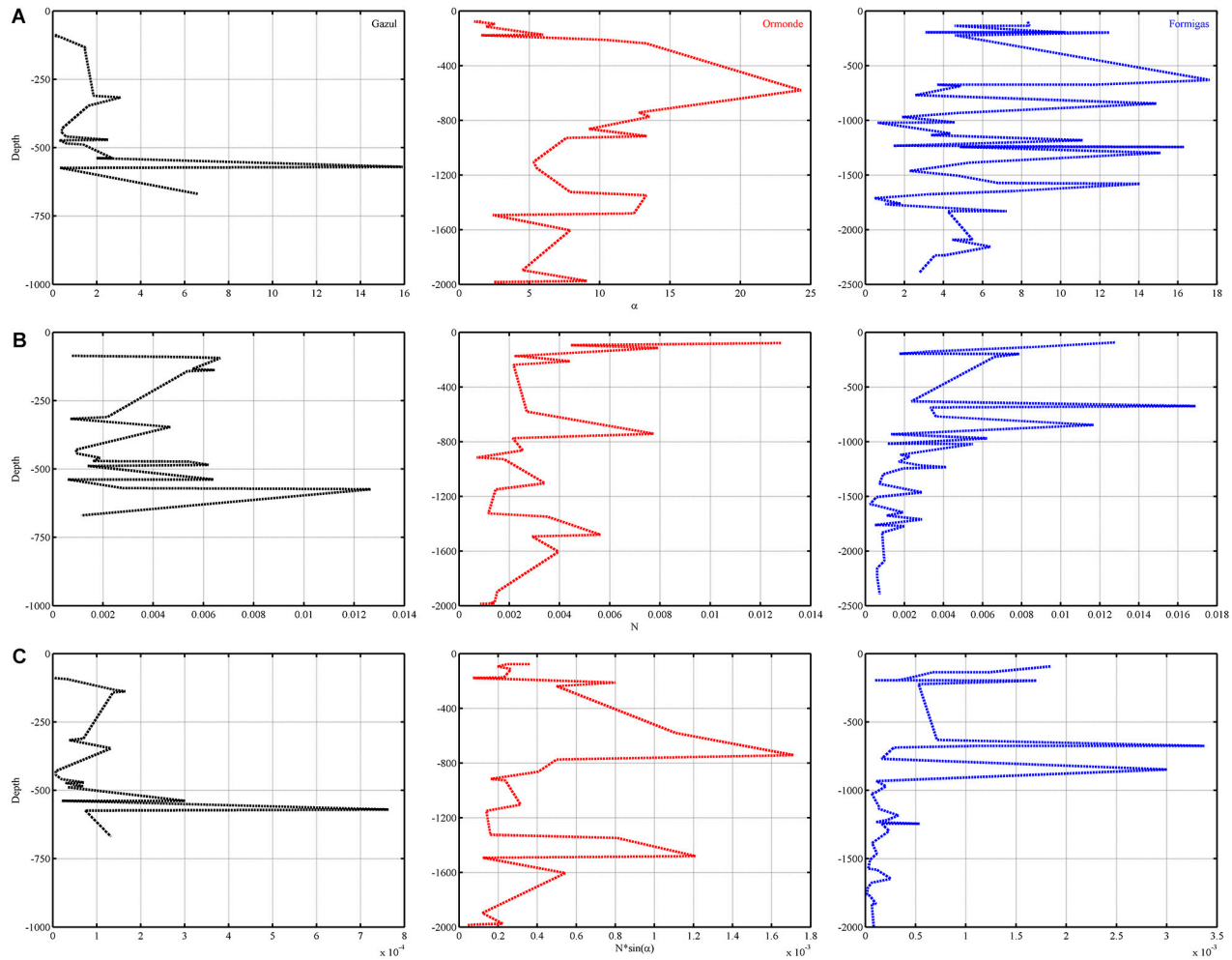

FIGURE 13 | Vertical profiles of (from top to bottom) angle of incline of the seabed **(A)**, Brunt–Väisälä frequency **(B)**, and parameter $N^*\sin(\alpha)$ **(C)** for (from left to right) the Gazul mud volcano (in black), and the Ormonde (in red), and the Formigas (in blue) seamounts.

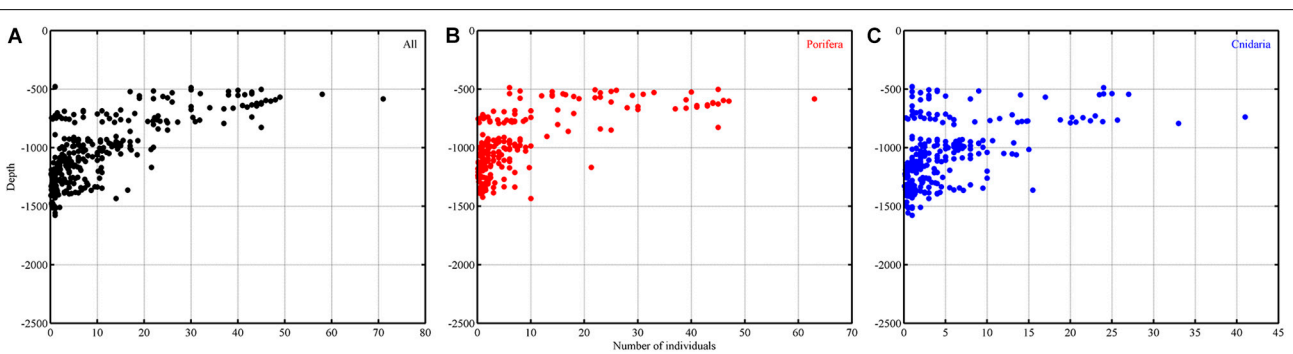

FIGURE 14 | Vertical profiles representing the abundance of benthic invertebrates averaged in 2 m bins for all phyla **(A)**, porifera **(B)**, and cnidaria **(C)** in Formigas seamount. The gray dashed line represents the coefficient between the bottom slope and the angle of propagation of the internal waves (γ/c).

formation during the time when the *in situ* observations were gathered. Furthermore, the seasonality and fluctuation of the flow as indicated by the climatological data (**Figure 3**) lead us to suggest that this particular phenomenon, as well as any other related with a constant flow (i.e., current deflection, turbulence, and persistent upwelling) in case they take place, will not last for long periods due to the variability of the currents. Moreover, the barotropic tides in the regions of study show values comparable

to the ocean currents, particularly in Ormonde, and Formigas, and hence they will override the residual circulation that could be induced by Taylor caps.

The permanent layout of water masses distribution through the water column suggests that the propagation of internal waves could be frequent. The density gradient is a determining factor for the generation and propagation of internal waves (Munk, 1981; Apel, 2004). Therefore, the hydrographical analysis of each one of the studied features allowed us to determine if internal waves might take place and how they would interact with the slope of the seamounts. The vertical distribution of the water masses, and in particular, the presence of the MOW, with its associated salinity gradient, determines the stratification of the water column. The analyses of the vertical distribution of the water masses in each of the three features show an intense stratification at mid-depths in the three regions studied, as it is indicated by the relatively high values of the Brunt–Väisälä frequency. This intense stratification is due to the density difference between the Atlantic and Mediterranean waters, which determines the stability of the water column. The associated high values of the Brunt–Väisälä frequency make the NACW–MOW interface an adequate area for the generation and propagation of internal waves, which after the interaction with the gentle slope of the seamounts, can end up breaking, and therefore enhancing the vertical mixing and producing upwelling (IUCN, 2013; Rivera et al., 2016).

Moreover, at the latitude of the regions of study, poleward 30°N, waves traveling at diurnal periods may be trapped over the slope, generating amplified currents at the depths where N is maximum, i.e., in the interface generated by the presence of the MOW, and as indicated by the barotropic tides, with enough energy for the development of internal waves (White and Dorschel, 2010).

White and Dorschel (2010) proposed that a stable stratification could help the growth of CWC on regions of enhanced energy near the sea bottom. It is in this region of maximum energy, in the interface associated to the presence of the MOW (500–1,000 m), where we have found the higher abundance of benthic suspension feeders in the Formigas seamount (**Figure 14**), particularly invertebrates such as poriferans and cnidarians. Specifically, two relative maxima coincide with critical values of the γ/c relationship, one at the NACW–MOW interface and another at the MOW core; and a third relative maximum is around 1,200 m, due to the MOW–NADW interface. The presence of suspension feeders on the slopes of seamounts has been largely attributed to the activity of internal waves (Frederiksen et al., 1992; Duineveld et al., 2004; De Mol et al., 2005; Mienis et al., 2007; Davies et al., 2009; van Haren et al., 2017). Frederiksen et al. (1992) suggested that corals living on deep waters cannot only be supported by the scarce supply of food coming from the surface layers. Instead, they postulated that the intensification of the mixing at the bottom, due to the interaction of internal waves with a sloping bottom, would produce the mobilization of the organic material deposited on the seabed, enhancing food supply for benthic organisms. The favorable effects caused by internal waves have already been observed in the CWC reefs dominated by the coral *Lophelia pertusa* in areas of the Northeast Atlantic as the Mingulay Reef complex (Davies et al., 2009), Tisler Reef (Wagner et al., 2011), and the Logachev Mounds at Rockall Bank (Duineveld et al., 2007; Soetaert et al., 2016). These processes could favor the settlement and growth of CWC and other benthic taxa on areas of steep topography, such as the slope of the seamounts. The presence of the MOW at mid-depths guarantees a permanent stratification that allows the generation and propagation of internal waves.

We have demonstrated that there is a strong relation between the NACW–MOW interface, associated with the activity of internal waves, and the abundance of benthic suspension feeders. This supports the hypothesis that the biological importance of seamounts in the pathway of the MOW through the eastern Atlantic (WWF, 2004; Oceana, 2005; Rueda et al., 2016) might be associated to internal waves in the NACW–MOW interface, that improves the favorable conditions for benthic suspension feeders to grow on the slope of the seafloor elevations.

AUTHOR CONTRIBUTIONS

PV-B and CO conceived and designed the research. CO, PV-B, JR, SP, VC, and JJ performed the field work. ÁM, PV-B, and SP processed the oceanographic data and elaborated the preliminary results. CD-C and JB-F processed the video transects and provided the video biological data. ÁM, PP, and CO processed the video biological data. ÁM, PV-B, RB, JR, and NF contributed to the further analysis of data. ÁM and PV-B wrote the manuscript. JR, SP, VC, PP, and CO revised the manuscript and contributed to the writing. CD-C, MC-S, and TM contributed to the writing associated with the biological data.

FUNDING

This work is a contribution to the ATLAS project and has received funding from the European Union's Horizon 2020 Research and Innovation Program under grant agreement no. 678760.

ACKNOWLEDGMENTS

The Roemmich-Gilson Argo Climatology is freely available from http://sio-argo.ucsd.edu/. Drifter Data and Products are accessible for free at http://www.aoml.noaa.gov/, courtesy of NOAA's Climate Program Office. NOAA High Resolution SST and ICOADS data are provided by the NOAA/OAR/ESRL PSD, Boulder, CO, United States, from their website at https://www.esrl.noaa.gov/psd/. Data from the barotropic tide model TXPO7.2 can be free downloaded at http://volkov.oce.orst.edu/tides/. SP acknowledges predoctoral FPI Fellowship (BES-2015-074316) support from the Spanish Ministry of Economy and Competitiveness, co-funded by the European Social Fund. This article is a publication of the Unidad Océano y Clima of the Universidad de Las Palmas de Gran Canaria, a R&D&i CSIC-associate unit.

REFERENCES

Apel, J. R. (2004). "Oceanic Internal Waves and Solitons," in *Synthetic Aperture Radar marine User's Manual*, eds C. R. Jackson, and J. R. Apel, (Washington DC: U.S. Department of Commerce), 189–206.

Bashmachnikov, I., Mohn, C., Pelegrí, J. L., Martins, A., Jose, F., Machín, F., et al. (2009). Interaction of Mediterranean water eddies with Sedlo and Seine Seamounts, Subtropical Northeast Atlantic. *Deep Sea Res. II Top. Stud. Oceanogr.* 56, 2593–2605. doi: 10.1016/j.dsr2.2008.12.036

Bashmachnikov, I., Nascimento, Â, Neves, F., Menezes, T., and Koldonov, N. V. (2015). Distribution of intermediate water masses in the Subtropical Northeast Atlantic. *Ocean Sci.* 11, 803–827. doi: 10.5194/os-11-803-2015

Beckmann, A., and Mohn, C. (2002). The upper ocean circulation at Great Meteor Seamount. Part II: Retention potential of the seamount-induced circulation. *Ocean Dyn.* 52, 194–204. doi: 10.1007/s10236-002-0018-3

Boehlert, G., and Genin, A. (1987). "A review of the effects of seamounts on biological processes," in *Seamounts, Islands and Atolls*, eds B. H. Keating, et al. (Washington DC: American Geophysical Union), 319–334. doi: 10.1029/gm043p0319

Bozec, A., Lozier, M. S., Chassignet, E. P., and Halliwell, R. (2011). On the variability of the Mediterranean Outflow Water in the North Atlantic from 1948 to 2006. *J. Geophys. Res.* 116:C09033. doi: 10.1029/2011JC007191

Brenke, N. (2002). The benthic community of the Great Meteor Bank. Oceanography and Ecology of Seamounts – Indications of Unique Ecosystems. *ICS ASC CM 2002/M-30*. Copenhagen 12.

Cacchione, D., and Wunsch, C. (1974). Experimental study of internal waves over a slope. *J. Fluid Mech.* 66, 223–239. doi: 10.1017/S0022112074000164

Clark, M. R., Rowden, A. A., Schlacher, T., Williams, A., Consalvey, M., Stocks, K. I., et al. (2010). The ecology of seamounts: structure, function, and human impacts. *Annu. Rev. Mar. Sci.* 2, 253–278. doi: 10.1146/annurev-marine-120308-081109

Coelho, E., and Santos, R. (2003). Enhanced primary production over seamounts: A numerical study. *Thalassas* 19, 144–145.

Comas-Rodríguez, I., Hernández-Guerra, A., and McDonagh, E. L. (2010). Referencing geostrophic velocities using ADCP data at 24.5°N (North Atlantic). *Sci. Mar.* 74, 331–338. doi: 10.3989/scimar.2010.74n2331

Daniault, N., Mazé, J. P., and Arhan, M. (1994). Circulation and mixing of Mediterranean Water west of the Iberian Peninsula. *Deep Sea Res. I Oceanogr. Res. Pap.* 41, 1685–1714. doi: 10.1016/0967-0637(94)90068-X

Davies, A. J., Duineveld, G. C. A., Lavaleye, M. S. S., Bergman, M. J. N., van Haren, H., and Roberts, J. M. (2009). Downwelling and deep-water bottom currents as food supply mechanisms to the cold-water coral *Lophelia pertusa* (*Scleractinia*) at the Mingulay Reef complex. *Limnol. Oceanogr.* 54, 620–629. doi: 10.4319/lo.2009.54.2.0620

De Mol, B., Henriet, J.-P., and Canals, M. (2005). "Development of coral banks in Porcupine Seabight: do they have Mediterranean ancestors?" in *Cold-water Corals and Ecosystems*, eds A. Freiwald, and J. M. Roberts, (Springer: Berlin Heidelberg), 515–533. doi: 10.1007/3-540-27673-4_26

De Mol, B., Van Rensbergen, P., Pillen, S., Van Herreweghe, K., Van Rooij, D., McDonnell, A., et al. (2002). Large deep-water coral banks in the Porcupine Basin, southwest of Ireland. *Mar. Geol.* 188, 193–231. doi: 10.1016/S0025-3227(02)00281-5

Denda, A., Mohn, C., Wehrmann, H., and Christiansen, B. (2016). Microzooplankton and meroplanktonic larvae at two seamounts in the subtropical and tropical NE Atlantic. *J. Mar. Biol. Assoc. U.K.* 97, 1–27. doi: 10.1017/S0025315415002192

Dower, J., Freeland, H., and Juniper, K. (1992). A strong biological response to oceanic flow past Cobb Seamount. *Deep Sea Res. A Oceanogr. Res. Pap.* 39, 1139–1145. doi: 10.1016/0198-0149(92)90061-W

Duineveld, G. C. A., Lavaleye, M. S. S., and Berghuis, E. M. (2004). Particle flux and food supply to a seamount cold-water coral community (Galicia Bank. NW Spain). *Mar. Ecol. Prog. Ser.* 277, 13–23. doi: 10.3354/meps277013

Duineveld, G. C. A., Lavaleye, M. S. S., Bergman, M. J. N., de Stigter, H., and Mienis, F. (2007). Trophic structure of a cold-water coral mound community (Rockall Bank. NE Atlantic) in relation to the near-bottom particle supply and current regime. *Bull. Mar. Sci.* 81, 449–467.

Egbert, G. D., and Erofeeva, S. Y. (2002). Efficient inverse modeling of barotropic ocean tides. *J. Atmos. Ocean. Technol.* 19, 183–204. doi: 10.1175/1520-04262002019<0183:EIMOBO<2.0.CO;2

Eriksen, C. C. (1991). Observations of amplified flows atop a large seamount. *J. Geophys. Res.* 96, 15227–15236. doi: 10.1029/91JC01176

Fischer, J., and Visbeck, M. (1993). Deep velocity profiling with self-contained AD. *J. Atmos. Ocean. Technol.* 10, 764–773. doi: 10.1175/1520-04261993010<0764:DVPWSC<2.0.CO;2

Frederiksen, R., Jensen, A., and Westerberg, H. (1992). The distribution of the scleractinian coral Lophelia pertusa around the Faroe islands and the relation to internal tidal mixing. *Sarsia* 77, 157–171. doi: 10.1080/00364827.1992.10413502

Gubbay, S. (2003). *Seamounts of the North-East Atlantic*. Burlington: OASIS.

Hall, R. A., Huthnance, J. M., and Williams, R. G. (2013). Internal wave reflection on shelf slopes with depth-varying stratification. *J. Phys. Oceanogr.* 43, 248–258. doi: 10.1175/JPO-D-11-0192.1

Henry, L.-A., Frank, N., Hebbeln, D., Wienberg, C., Robinson, L., van de Flierdt, T., et al. (2014). Global ocean conveyor lowers extinction risk in the deep sea. *Deep Sea Res. I Oceanogr. Res. Pap.* 88, 8–16. doi: 10.1016/j.dsr.2014.03.004

Huthnance, J. M. (1981). Waves and currents near the continental shelf edge. *Prog. Oceanogr.* 10, 193–226. doi: 10.1016/0079-6611(81)90004-5

Iorga, M. C., and Lozier, M. S. (1999). Signatures of the Mediterranean outflow from a North Atlantic climatology 1. Salinity and density fields. *J. Geophys. Res.* 104, 25985–26009. doi: 10.1029/1999JC900115

IUCN, (2013). *Seamounts Project: An Ecosystem Approach to Management of Seamounts in the Southern Indian Ocean*. Switzerland: International Union for Conservation of Nature.

Johnson, J., and Stevens, I. (2000). A fine resolution model of the eastern North Atlantic between the Azores, the Canary Islands and the Gibraltar Strait. *Deep Sea Res. I Oceanogr. Res. Pap.* 47, 875–899. doi: 10.1016/S0967-0637(99)00073-4

Juliano, M. F., and Alves, M. L. G. R. (2007). The Atlantic Subtropical Front/Current Systems of Azores and St. Helena. *J. Phys. Oceanogr.* 37, 2573–2598. doi: 10.1175/2007JPO3150.1

Koslow, J. A., Gowlett-Holmes, K., Lowry, J. K., Hara, T. O., Poore, G. C. B., and Williams, A. (2001). Seamount benthic macrofauna off southern Tasmania: Community structure and impacts of trawling. *Mar. Ecol. Prog. Ser.* 213, 111–125. doi: 10.3354/meps213111

Lavelle, J. W., and Mohn, C. (2010). Motion, commotion, and biophysical connections at deep ocean seamounts. *Oceanography* 23, 90–103. doi: 10.5670/oceanog.2010.64

Lumpkin, R., and Johnson, G. C. (2013). Global ocean surface velocities from drifters: Mean, variance. El Niño-Southern Oscillation response, and seasonal cycle. *J. Geophys. Res. Oceans* 118, 2992–3006. doi: 10.1002/jgrc.20210

Mienis, F., de Stigter, H. C., White, M., Duineveld, G., de Haas, H., and van Weering, T. C. E. (2007). Hydrodynamic controls on cold-water coral growth and carbonate-mound development at the SW and SE Rockall Trough Margin. NE Atlantic Ocean. *Deep Sea Res. I Oceanogr. Res. Pap.* 54, 1655–1674. doi: 10.1016/j.dsr.2007.05.013

Miller, K. J., and Gunasekera, R. M. (2017). A comparison of genetic connectivity in two deep sea corals to examine whether seamounts are isolated islands or stepping stones for dispersal. *Sci. Rep.* 7:46103. doi: 10.1038/srep46103

Mohn, C., and Beckmann, A. (2002). The upper ocean circulation at Great Meteor Seamount. Part I: Structure of density and flow fields. *Ocean Dyn.* 52, 179–193. doi: 10.1007/s10236-002-0017-4

Munk, W. (1981). "Internal Waves and Small-scale Processes," in *Evolution of Physical Oceanography*, eds B. A. Warren, and C. Wunsch, (Cambridge, MA: The MIT Press), 264–291.

Noble, M., and Mullineaux, L. (1989). Internal tidal currents over the summit of Cross Seamount. *Deep Sea Res. A Oceanogr. Res. Pap.* 36, 1791–1802. doi: 10.1016/0198-0149(89)90112-X

Oceana. (2005). *The Seamounts of the Gorringe Bank*. Milan: Fondazione Ermenegildo Zegna, 74.

O'Hara, T. (2007). Seamounts: centres of endemism or species richness for ophiuroids? *Glob. Ecol. Biogeogr.* 16, 720–732. doi: 10.1111/j.1466-8238.2007.00329.x

O'Hara, T. D., Rowden, A. A., and Williams, A. (2008). Cold-water coral habitats on seamounts: do they have a specialist fauna? *Divers. Distrib.* 14, 925–934. doi: 10.1111/j.1472-4642.2008.00495.x

Orejas, C., Addamo, A., Álvarez, M., Aparicio, A., Alcoverro, D., Arnaud-Haond, S., et al. (2017). *Cruise Summary Report - MEDWAVES survey. (MEDiterranean out flow WAter and Vulnerable EcosystemS)*. doi: 10.5281/zenodo.556516

Palomino, D., López-González, N., Vázquez, J. T., Fernández-Salas, L. M., Rueda, J. L., González-García, E., et al. (2015). "Volumen De Comunicaciones Presentadas En El VIII Simposio Sobre El Margen Ibérico Atlántico" in *Características Geológicas, Oceanográficas y Bentónicas del Volcán de Fango Gazul en el Talud Medio del Golfo de Cádiz* eds V. Díaz del Río, P. Bárcenas, L. M. Fernández-Salas, (Madrid: Instituto Español de Oceanografía) 157–160.

Palomino, D., Vázquez, J. T., Somoza, L., León, R., López-González, N., Medialdea, T., et al. (2016). Geomorphological features in the southern Canary Island Volcanic Province: The importance of volcanic processes and massive slope instabilities associated with seamounts. *Geomorphology* 255, 125–139. doi: 10.1016/j.geomorph.2015.12.016

Pitcher, T. J., Morato, T., Hart, P. J. B., Clark, M. R., Haggan, N., and Santos, R. S. (2007). "The depths of ignorance: an ecosystem evaluation framework for seamount ecology, fisheries and conservation" in *Seamounts: ecology, fisheries & conservation (Fish and Aquatic Resources Series, 12)*, ed. T. J. Pitcher, et al. (Oxford: Blackwell Science), 446–497.

Relvas, P., Barton, E. D., Dubert, J., Oliveira, P. B., Peliz, A., da Silva, J. C. B., et al. (2007). Physical oceanography of the western Iberia ecosystem: Latest views and challenges. *Prog. Oceanogr.* 74, 149–173. doi: 10.1016/j.pocean.2007.04.021

Reynolds, R. W., Smith, T. M., Liu, C., Chelton, D. B., Casey, K. S., and Schlax, M. G. (2007). Daily high-resolution-blended analyses for sea surface temperature. *J. Climate* 20, 5473–5496. doi: 10.1175/2007JCLI1824.1

Rivera, J., Canals, M., Lastras, G., Hermida, N., Amblas, D., Arrese, B., et al. (2016). Morphometry of Concepcion Bank: Evidence of Geological and Biological Processes on a Large Volcanic Seamount of the Canary Islands Seamount Province. *PLoS One* 11:e0156337. doi: 10.1371/journal.pone.0156337

Roden, G. I. (1986). "Aspects of oceanic flow and thermohaline structure in the vicinity of seamounts", in *Environment and Resources of Seamounts in the North Pacific*, ed. R. N. Uchida, S. Hayasi, and G. W. Boehlert, (Washington DC: U. S Department of Commerce), 3–12

Roden, G. I. (1991). Mesoscale flow and thermohaline structure around Fieberling Seamount. *J. Geophys. Res.* 96, 16653–16672. doi: 10.1029/91JC01747

Roemmich, D., and Gilson, J. (2009). The 2004-2008 mean and annual cycle of temperature, salinity, and steric height in the global ocean from the Argo Program. *Prog. Oceanogr.* 82, 81–100. doi: 10.1016/j.pocean.2009.03.004

Royer, T. C. (1978). Ocean eddies generated by seamounts in the North Pacific. *Science* 199, 1063–1064. doi: 10.1126/science.199.4333.1063-a

Rueda, J. L., González-García, E., Krutzky, C., López-Rodríguez, F. J., Bruque, G., López-González, N., et al. (2016). From chemosynthesis-based communities to cold-water corals: Vulnerable deep-sea habitats of the Gulf of Cadiz. *Mar. Biodiv.* 46, 473–482. doi: 10.1007/s12526-015-0366-0

Rueda, J. L., Urra, J., Gofas, S., López-González, N., Fernández-Salas, L. M., and Díaz-Del-Río, V. (2012). New records of recently described chemosymbiotic bivalves for mud volcanoes within the European waters (Gulf of Cádiz). *Mediterr. Mar. Sci.* 13, 262–267. doi: 10.12681/mms.307

Sala, I., Harrison, C. S., and Caldeira, R. M. A. (2016). The role of the Azores Archipelago in capturing and retaining incoming particles. *J. Mar. Syst.* 154, 146–156. doi: 10.1016/j.jmarsys.2015.10.001

Samadi, S., Bottan, L., Macpherson, E., Richer, de Forges, B., and Boissilier, M. C. (2006). Seamount endemism questioned by the geographic distribution and population genetic structure of marine invertebrates. *Mar. Biol.* 149, 1463–1475. doi: 10.1007/s00227-006-0306-4

Serrano, A., González-Irusta, J. M., Punzón, A., García-Alegre, A., Lourido, A., Ríos, P., et al. (2017). Deep-sea benthic habitats modeling and mapping in a NE Atlantic seamount (Galicia Bank). *Deep Sea Res.I Oceanogr. Res. Pap.* 126, 115–127. doi: 10.1016/j.dsr.2017.06.003

Soetaert, K., Mohn, C., Rengstorf, A., Grehan, A., and van Oevelen, D. (2016). Ecosystem engineering creates a direct nutritional link between 600-m deep cold-water coral mounds and surface productivity. *Sci. Rep.* 6:35057. doi: 10.1038/srep35057

Sokolovskiy, M. A., Filyushkin, B. N., and Carton, X. J. (2013). Dynamics of intrathermocline vortices in a gyre flow over a seamount chain. *Ocean Dyn.* 63, 741–760. doi: 10.1007/s10236-013-0628-y

Staudigel, H., Koppers, A. A. P., Lavelle, J. W., Pitcher, T. J., and Shank, T. M. (2010). Box 1: Defining the word "seamount". *Oceanography* 23, 20–21. doi: 10.5670/oceanog.2010.85

van Haren, H., Hanz, U., de Stigter, H., Mienis, F., and Duineveld, G. (2017). Internal wave turbulence at a biologically rich Mid-Atlantic seamount. *PLoS One* 12:e0189720. doi: 10.1371/journal.pone.0189720

Wagner, H., Purser, A., Thomsen, L., Jesus, C. C., and Lundälv, T. (2011). Particulate organic matter fluxes and hydrodynamics at the Tisler cold-water coral reef. *J. Mar. Syst.* 85, 19–29. doi: 10.1016/j.jmarsys.2010.11.003

White, M., and Dorschel, B. (2010). The importance of the permanent thermocline to the cold water coral carbonate mound distribution in the NE Atlantic. *Earth Planet. Sci. Lett.* 296, 395–402. doi: 10.1016/j.epsl.2010.05.025

WWF, (2004). *Cold-Water Corals: Fragile Havens in the Deep*. Switzerland: WWF.

Xavier, J., and van Soest, R. (2007). Demosponge fauna of Ormonde and Gettysburg Seamounts (Gorringe Bank, north-east Atlantic): Diversity and zoogeographical affinities. *J. Mar. Biolog. Assoc. U.K.* 87, 1643–1653. doi: 10.1017/S0025315407058584

Conflict of Interest: The authors declare that the research was conducted in the absence of any commercial or financial relationships that could be construed as a potential conflict of interest.